 Bull. Chem. Soc. Jpn., **76**, 153–162 (2003)

Kinetic Analysis of the Cleavage of the Ribose Phosphodiester Bond within Guanine and Cytosine-Rich Oligonucleotides and Dinucleotides at 65–200 °C and Its Implications Concerning the Chemical Evolution of RNA

Kunio Kawamura*

Department of Applied Chemistry, Osaka Prefecture University, Gakuen-cho 1-1, Sakai, Osaka 599-8531

(Received April 30, 2002)

A monitoring method of rapid hydrothermal reactions was successfully applied to a kinetic analysis of the cleavage of a ribose phosphodiester bond within oligonucleotides and dinucleotides at 150–200 °C. The apparent rate constants (k_{app}) of degradation of the ribose 3′,5′-cytidylylguanosine sequence (-$C^{3'}pG_d$-) within oligonucleotides and dinucleotides were determined, where the -$C^{3'}pG_d$- sequence in oligonucleotides is less stable than 2′,5′-cytidylylguanosine ($C^{2'}pG$) and 3′,5′-cytidylylguanosine ($C^{3'}pG$). It was unexpected that the stability of the target sequence would be dependent on the surrounding sequences of the oligonucleotides, although the temperatures used in the study were extremely higher than the melting points. The stability of a phosphodiester bond of 2′-deoxycytidylyl-2′-deoxyguanosine (C_dpG_d) is much higher than that of a ribose phosphodiester bond at low temperatures, but becomes comparable at 200 °C. During the degradation of $C^{2'}pG$ or $C^{3'}pG$, interconversion between $C^{2'}pG$ and $C^{3'}pG$ was observed along with cleavage of the phosphodiester bond. Based on an analysis of the extent of interconversion, the apparent rate constants of the disappearance of $C^{2'}pG$ and $C^{3'}pG$ were dissected into the rate constants of hydrolysis (k_{hy}) and interconversion (k_{int}), where the values of k_{hy} were greater than those of k_{int}. The apparent activation energy of the degradation of the target sequence was 100–109 kJ mol^{-1} for oligonucleotides, 90 kJ mol^{-1} for $C^{3'}pG$, and 87 kJ mol^{-1} for $C^{2'}pG$, and 139 kJ mol^{-1} for C_dpG_d. The apparent activation enthalpy and entropy changes of the degradation of the target sequence were also determined; the values of the activation parameter were $\Delta H^{\neq}_{app}$ = 94–105 kJ mol^{-1} and $\Delta S^{\neq}_{app}$ = −(36–59) J mol^{-1} T^{-1} for five oligonucleotides, $\Delta H^{\neq}_{app}$ = 86 kJ mol^{-1} and $\Delta S^{\neq}_{app}$ = −97 J mol^{-1} T^{-1} for $C^{3'}pG$, $\Delta H^{\neq}_{app}$ = 84 kJ mol^{-1}, $\Delta S^{\neq}_{app}$ = −105 J mol^{-1} T^{-1} for $C^{2'}pG$, and $\Delta H^{\neq}_{app}$ = 135 kJ mol^{-1}, $\Delta S^{\neq}_{app}$ = +2 J mol^{-1} T^{-1} for C_dpG_d. The activation parameters, $\Delta H^{\neq}_{app}$ and $\Delta S^{\neq}_{app}$, for the oligonucleotides increased with the length of the surrounding sequence of -$C^{3'}pG_d$-; this fact clearly demonstrates the existence of the influence of the surrounding sequence for the stability of the target ribose phosphodiester bond. Based on a kinetic analysis, the reaction mechanism of the degradation of the ribose phosphodiester bond at high temperatures is discussed. Furthermore, possible pathways of the chemical evolution of RNA are discussed from the viewpoint of the hydrothermal origin of life.

Hydrothermal systems, such as hydrothermal vents in the deep ocean, have played important roles concerning the emergence of life under the primitive earth conditions (the hydrothermal origin of life hypothesis).[1–3] For instance, there have been a few studies that demonstrate possible pathways for the formation of biologically important molecules, such as proteins.[4–6] Phylogenetic analyses indicate that the last common ancestor of all present organisms had the nature of hyperthermophiles.[7,8] On the other hand, the discovery of the catalytic activity of RNA suggests that RNA played central roles in the emergence of life under primitive earth environments.[9,10] The RNA world hypothesis is supported by studies on spontaneous RNA formation[11–15] and the in vitro selection of RNA.[16] However, the low stability of RNA at high temperatures seems to be in conflict with the hydrothermal origin-of-life hypothesis.[17–24] Thus, we have been carrying out investigations on the RNA world hypothesis based on views concerning the hydrothermal origin of life.[19–26] During these investigations, we were confronted with the difficulty on monitoring the reactions in real time at high temperatures of over 100 °C, since the reactions are very rapid. In general, because the real-time monitoring of hydrothermal reactions was difficult or impossible, the extrapolation of Arrhenius plots determined at low temperatures was necessary to estimate the reaction rates in aqueous solution at high temperatures. To solve this problem, we recently developed a new monitoring method of hydrothermal reactions.[21–23]

Furthermore, there have been a number of studies on the hydrolytic stability of the ribose phosphodiester bond with and without imidazole as a ribonuclease model.[27–42] However, fewer studies were carried out on the temperature dependence and stability at extremely high temperatures.[30]

The present study is the first systematic investigation on the stability of the ribose phosphodiester bond at high temperatures of over 100 °C using a new monitoring method.[24] At temperatures of 150–200 °C, which are fairly higher than the melting points of the oligonucleotides, the difference in the stability of the target sequence, -$C^{3'}pG_d$-, was examined using oligonucleotides with different sequences.[24] The values of k_{app}

in the degradation of oligonucleotides at 150–200 °C were determined and compared with those at 65–80 °C. The k_{app} values of $C^{2'}pG$ and $C^{3'}pG$ were dissected into the rate constants of hydrolysis and interconversion between $C^{2'}pG$ and $C^{3'}pG$ to investigate the reaction mechanism. Furthermore, the kinetics and activation parameters determined from the temperature dependence of the rate constants support a reaction mechanism through a pentacoordinate phosphorane intermediate. This model was applied for the dinucleotides and oligonucleotides. Additionally, the stability of nucleic acids is discussed from the viewpoint of the hydrothermal origin of life.

Experimental

Chemicals. Five oligonucleotides with sequences 5′-$G_dG_dC_d$-$CG_dG_dT_dT_dT_dT_dC_dC_dG_dG_dC_dC_d$ (oligo-17), 5′-$G_dG_dC_dCG_dG_dT_dT_dT_dT_dT_d$ (oligo-11), 5′-$G_dG_dG_dC_dC_dCG_dG_dG_dT_dT_dT_dT_dC_dC_d$-$C_dG_dG_dG_dC_dC_dC_d$ (oligo-23), 5′-$G_dG_dC_dC_dG_dG_dT_dT_dCG_dT_dT_dC_d$-$C_dG_dG_dC_dC_d$ (oligo-18), and 5'-$C_dCG_dG_d$ (oligo-4) were purchased from GenSet (France) as HPLC purified grade. Authentic oligonucleotides, which correspond to the degradation products, were also obtained from GenSet. Dinucleoside monophosphates, $C^{2'}pG$, $C^{3'}pG$, and C_dpG_d, were obtained from Sigma-Aldrich Japan (Tokyo, Japan). All other reagents were obtained from Sigma (St. Louis, MO, USA) and Wako (Osaka, Japan).

Apparatus. The monitoring system for hydrothermal reactions was set up as described in previous studies.[21–23] The system consists of a 1 L (1 L = 1 dm^3) H_2O reservoir, a high-pressure HPLC pump (model PU-980, JASCO Corporation, Japan), a sample injector (Rheodyne, with 0.1 mL sample loop), a hydrothermal reactor, a cooling bath, and a back-pressure tubing, a sampling port, and a temperature controller. The system was connected with transfer lines (0.1 mm inner diameter (ID) of stainless-steel (SUS) tubing), and double-distilled water, which was filtered with a 0.2 μm membrane filter, and pumped from the reservoir against the back pressure on the system. The pressure in the reactor was regulated using back-pressure tubing at 10 M Pa. The flow reactor consisted of tubing and a heating block, in which the temperature was controlled at ±1%. Poly(oxy-1,4-phenyleneoxy-1,4-phenylenecarbonyl-1,4-phenylene) (PEEK) and poly(tetrafluoroethylene) (PTFE) tubing with 0.13 or 0.25 mm inner diameter (ID) were tested. The residence time exposed at high temperature was controlled by changing the flow rate of the pump at 0.05–2 mL min^{-1} and using different sizes of tubing. The effective inner volumes of tubing were determined by weighing with and without filling water at 25 °C.

Sample Preparation and Kinetic Analysis. Sample solutions containing 5×10^{-5} M (1 M = 1 mol dm^{-3}) nucleotide, 0.1 M NaCl, 0.1 M $MgCl_2$, and 0.05 M imidazole were prepared and the pH was adjusted to 8.0 with 0.01 M HCl or 0.01 M NaOH solutions at 25 °C. A 0.1 mL of the sample solution was injected to the flow system, and the sample exposed at a high temperature was withdrawn from the sampling port at an appropriate time period after sample injection and immediately quenched to 0 °C. High-performance liquid chromatography (HPLC) was carried out by a HPLC system LC10A (Shimadzu, Japan) with a DNA-NPR anion-exchange column from TOSOH Co., Japan using a gradient of 0.2–1.0 M NaCl at pH 9 with a 0.01 M 2-amino-2-hydroxymethyl-1,3-propanediol (Tris) buffer for oligo-17, -11, -18, and -23 and a ODS-2 column from GL Science Co., Japan using a gradient of 0.02 M NaH_2PO_4 and 0.005 M tetrabutylammonium bromide (TBABr) in water at pH 3.5 mixed with 0.02 M NaH_2PO_4 and 0.005 M TBABr in 60% CH_3OH at pH 3.5 for oligo-4, $C^{2'}pG$, $C^{3'}pG$, and C_dpG_d. A HPLC analysis was carried out at 35 °C and a wavelength of 260 nm was used for detection.

The melting temperatures (T_m) of oligo-17, -18, and -23 were determined using a CSC 6100 Nano II differential scanning calorimeter (DSC) (Calorimetry Sciences Corp., USA). Samples involving 0.75–1.0 mg of oligonucleotide in a 1 mL buffer solution were used for DSC analysis. The computer program SIMFIT was used to evaluate the rate constants.[15]

Results

Degradation of Oligonucleotides. There was no kinetic analysis in real-time on the hydrolytic stability of oligonucleotides under hydrothermal conditions until the present monitoring method was developed. In this study, five types of oligonucleotides, which involve a single phosphodiester bond in the -$C^{3'}pG_d$- sequence (Fig. 1), were selected for the following reasons. First, since the phosphodiester bond is cleaved more rapidly than DNA sequences, oligonucleotides begin to be divided into two sequences, as shown in Eqs. I-1 and I-2.[39,40,43,44] Thus, the stability of the target linkage -$C^{3'}pG_d$- (Fig. 1) can be assessed. Second, it is favorable to detect if a difference in the stability of the target linkage exists within different sequences, since intra- and inter-molecular interactions of guanine and cytosine-rich oligonucleotides are stronger than adenine and uracil-rich oligonucleotides. Third, guanine and cytosine-rich oligonucleotides are important from the view points of the chemical evolution of RNA, since primitive RNA was postulated to have guanine and cytosine-rich sequence[45] and oligonucleotides composed of guanine and cytosine are favorable to be replicated under primitive earth conditions without any enzymes.[11,15,26] The five types of sequence were chosen in order to understand the possible influences of the length of oligonucleotides, double- or single-strand, and hairpin or not.

The degradation of oligo-17 is visualized in the time course of HPLC charts in Fig. 2 and the reaction curves of the degra-

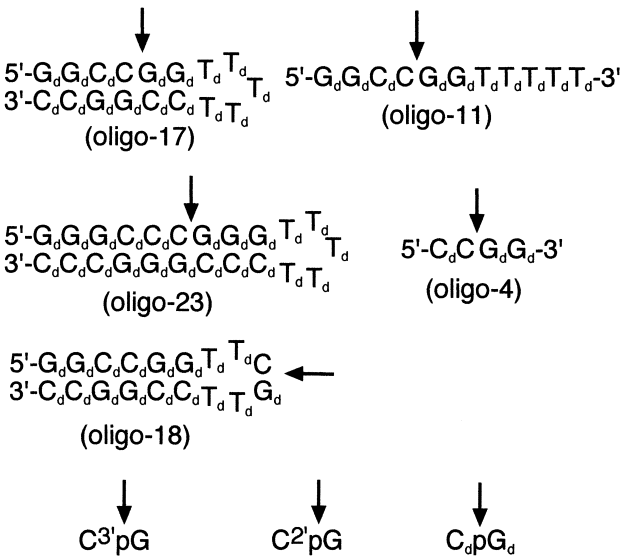

Fig. 1. Structures of oligonucleotides and dinucleotides used in the study. The arrow indicates ribose phosphodiester bond.

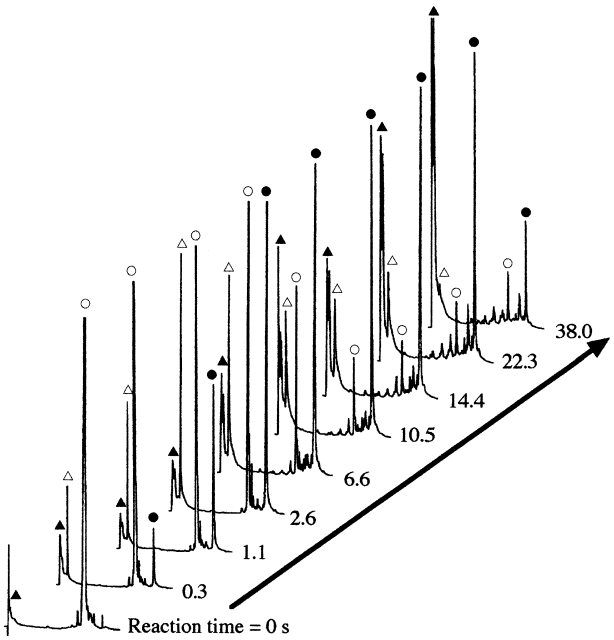

Fig. 2. HPLC profile during degradation of 5′-$G_dG_dC_d$-$CG_dG_dT_dT_dT_dT_dT_dC_dC_dG_dG_dC_dC_d$ (oligo-17) at 200 °C monitored by the present method. [NaCl] = 0.1 M, [$MgCl_2$] = 0.1 M, [imidazole] = 0.05 M, [oligo-17] = 5 × 10^{-5} M, pH = 8.0. ○: oligo-17, ●: 5′-$G_dG_dT_dT_dT_dT_d$-$T_dC_dC_dG_dG_dC_dC_d$, △: 5′-$G_dG_dC_dC$>p, ▲: monomers.

dation of oligonucleotides and dinucleotides are shown in Fig. 3. The reaction curves show that the degradation started within a few second at the position of the -$C^{3'}pG_d$- sequence to produce two oligonucleotides; they were then further hydrolyzed into monomer units. The interconversion of the ribose phosphodiester bond between 2′,5′- and 3′,5′-linkages in the five oligonucleotides was not detectable by HPLC, whereas the interconversion between $C^{2'}pG$ and $C^{3'}pG$ was observed (Fig. 4). Additionally, the degradation of the base moiety was not observed during the reactions. Thus, the reaction is expressed in Eqs. I-1 and I-2 for the case of oligo-17. The reaction model is expressed in general form for oligonucleotides and dinucleotides in Eqs. I-3 and I-4, since the original sequence is divided into two sequences:

$$\begin{aligned} &5'\text{-}G_dG_dC_dCG_dG_dT_dT_dT_dT_dC_dC_dG_dG_dC_dC_d \\ &\quad \rightarrow 5'\text{-}G_dG_dC_dC{>}p \\ &\qquad + 5'\text{-}G_dG_dT_dT_dT_dT_dT_dC_dC_dG_dG_dC_dC_d \qquad \text{(I-1)} \\ &\quad \rightarrow \text{monomers} \qquad \text{(I-2)} \\ &5'\text{-Seq(A)-Seq(B)} \rightarrow 5'\text{-Seq(A)}{>}p + 5'\text{-Seq(B)} \qquad \text{(I-3)} \\ &\qquad\qquad\qquad \rightarrow \text{monomers} \qquad \text{(I-4)} \end{aligned}$$

Here, 2′,3′-cyclic-phosphate of 5′-Seq(A)>p is to be further degraded to 5′-Seq(A) through 5′-Seq(A)-3′p and 5′-Seq(A)-2′p. Oligonucleotides from the reactions of oligo-11, -17, -18, and -23 were separated by anion-exchange HPLC. This method separates fractions based on the the number of negative charges on each oligonucleotide. The retention times of the products were assigned by co-injection with authentic oligonucleotides. It was interesting that the retention times of Seq(B) for oligo-17 and oligo-23, that is 5′-$G_dG_dT_dT_dT_dT_dT_dC_d$-$C_dG_dG_dG_dC_dC_d$ for oligo-17 and 5′-$G_dG_dG_dT_dT_dT_dT_dT_dC_dC_d$-$C_dG_dG_dG_dG_dC_dC_dC_d$ for oligo-23 are longer than those of oligo-17 and oligo-23. This is probably due to the formation of the hairpin form for oligo-17 and oligo-23.

The by-products, which possibly involve -$C^{3'}pG_d$- sequences, were less detected for the case of the five oligonucleotides. Moreover, the formation of monomers was relatively low at 65–150 °C. To eliminate the influence of the degradation of deoxyribose phosphodiester bond, the following correction (shown in Eq. I-5) was applied:

$$\begin{aligned} &-\mathrm{d}[5'\text{-Seq(A)-Seq(B)}]/\mathrm{d}t \\ &= -\mathrm{d}\{[5'\text{-Seq(A)-Seq(B)}]/([5'\text{-Seq(A)-Seq(B)}] \\ &\quad + [5'\text{-Seq(A)}{>}p] + [5'\text{-Seq(B)}])\}/\mathrm{d}t \qquad \text{(I-5)} \end{aligned}$$

For a kinetic analysis, the reaction curves at time ranges, at which the formation of monomers was negligible, were used. The first-order rate plots for the oligonucleotides and dinucleotides are consistent with a pseudo-first-order process (an example is shown in Fig. 5). The apparent rate constants (k_{app}) of the disappearance of oligonucleotides and dinucleotides were determined using a computer program, SIMFIT (Table 1). To evaluate the influence of the tubing material, PEEK and PTFE

Table 1. The Apparent Rate Constants (k_{app}/s^{-1}) of the Hydrolysis of Nucleotides at 65–200 °C

T/°C	65	80	150	175	200
Nucleotides					
oligo-4	$(1.02 \pm 0.02) \times 10^{-5}$	$(2.61 \pm 0.04) \times 10^{-5}$	$(1.01 \pm 0.01) \times 10^{-2}$	$(4.68 \pm 0.07) \times 10^{-2}$	$(2.21 \pm 0.02) \times 10^{-1}$
oligo-11	$(2.30 \pm 0.04) \times 10^{-5}$	$(4.47 \pm 0.06) \times 10^{-5}$	$(1.35 \pm 0.14) \times 10^{-2}$	$(7.30 \pm 0.06) \times 10^{-2}$	$(3.90 \pm 0.06) \times 10^{-1}$
oligo-17	$(4.85 \pm 0.08) \times 10^{-7}$	$(2.42 \pm 0.09) \times 10^{-5}$	$(7.15 \pm 0.12) \times 10^{-3}$	$(4.33 \pm 0.05) \times 10^{-2}$	$(2.92 \pm 0.04) \times 10^{-1}$
oligo-18	$(6.26 \pm 0.29) \times 10^{-6}$	$(2.57 \pm 0.06) \times 10^{-5}$	$(1.06 \pm 0.02) \times 10^{-2}$	$(4.89 \pm 0.18) \times 10^{-2}$	$(2.69 \pm 0.06) \times 10^{-1}$
oligo-23	$(6.61 \pm 0.30) \times 10^{-7}$	$(6.74 \pm 0.18) \times 10^{-6}$	$(1.09 \pm 0.04) \times 10^{-2}$	$(5.44 \pm 0.07) \times 10^{-2}$	$(2.92 \pm 0.04) \times 10^{-1}$
$C^{3'}pG$	$(3.67 \pm 0.14) \times 10^{-6}$	$(8.13 \pm 0.04) \times 10^{-6}$	$(1.27 \pm 0.02) \times 10^{-3}$	$(6.18 \pm 0.04) \times 10^{-3}$	$(3.22 \pm 0.02) \times 10^{-2}$
$C^{2'}pG$	$(3.73 \pm 0.17) \times 10^{-6}$	$(7.57 \pm 0.07) \times 10^{-6}$	$(1.10 \pm 0.01) \times 10^{-3}$	$(4.91 \pm 0.03) \times 10^{-3}$	$(2.44 \pm 0.02) \times 10^{-2}$
C_dpG_d	—	$(1.02 \pm 0.06) \times 10^{-7}$	$(2.04 \pm 0.24) \times 10^{-4}$	$(2.03 \pm 0.02) \times 10^{-3}$	$(1.73 \pm 0.02) \times 10^{-2}$
oligo-17[a)]	—	—	$(1.03 \pm 0.02) \times 10^{-2}$	$(4.86 \pm 0.06) \times 10^{-2}$	$(2.21 \pm 0.10) \times 10^{-1}$
oligo-17[b)]	—	—	$(1.00 \pm 0.01) \times 10^{-2}$	$(4.69 \pm 0.05) \times 10^{-2}$	$(2.14 \pm 0.06) \times 10^{-1}$

Reaction conditions: [nucleotide] = 5 × 10^{-5} M, [NaCl] = 0.1 M, [$MgCl_2$] = 0.1 M, [imidazole] = 0.05 M, pH = 8.0 (at 25 °C). The rate constants were determined by the flow method at 150–200 °C and by the batch method at 65–80 °C. a) 0.01 M L-histidine, b) 0.01 M D-histidine.

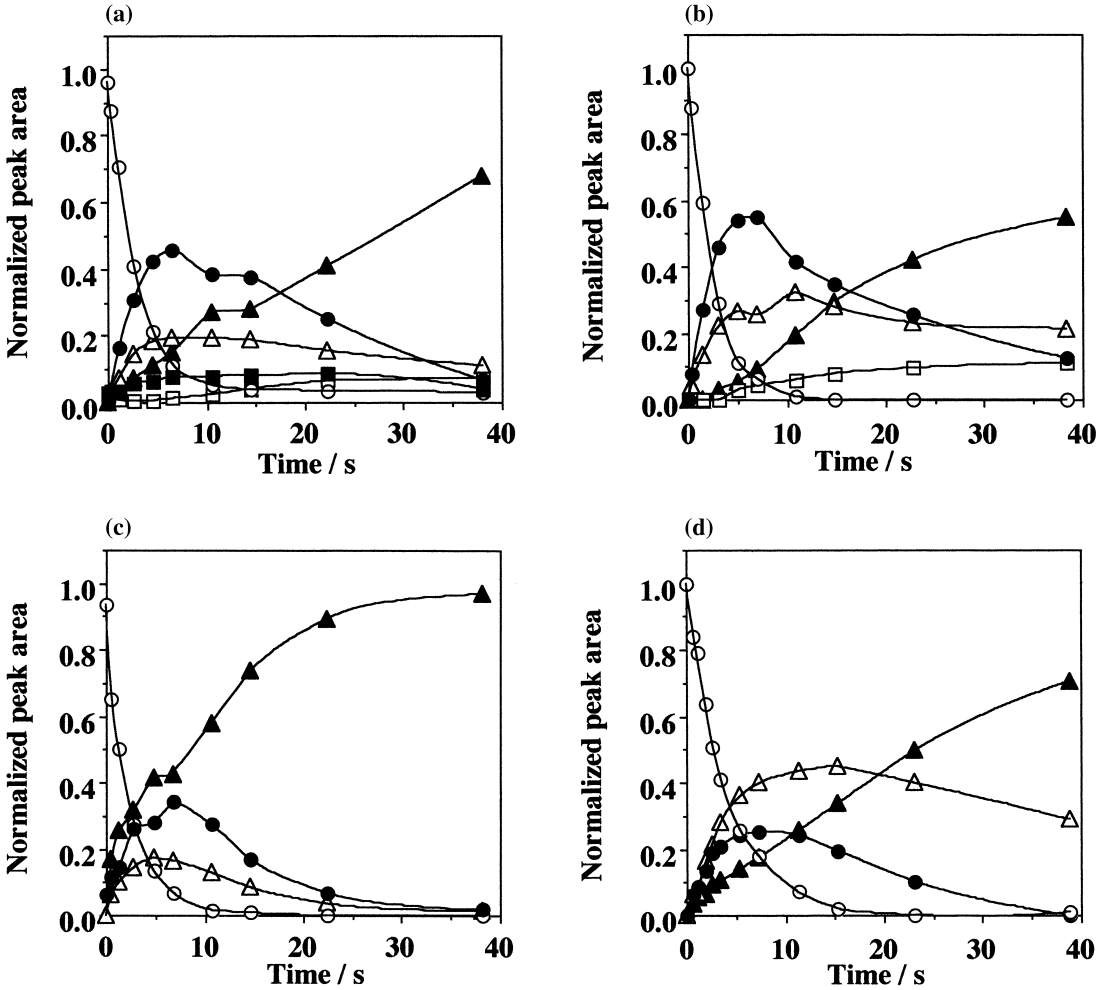

Fig. 3. Reaction curves for degradation of oligonucleotides. Reaction conditions: [NaCl] = 0.1 M, [$MgCl_2$] = 0.1 M, [imidazole] = 0.05 M, [oligonucleotide] = 5×10^{-5} M, pH = 8.0, temperature: 200 °C. (a) 5′-$G_dG_dC_dCG_dG_dT_dT_dT_dT_dC_dC_dG_dG_dC_dC_d$ (oligo-17), (b) 5′-$G_dG_dC_dCG_dG_dT_dT_dT_dT_dT_d$ (oligo-11), (c) 5′-$G_dG_dG_dC_dC_dCG_dG_dG_dT_dT_dT_dT_dC_dC_dC_dG_dG_dG_dC_dC_dC_d$ (oligo-23), (d) 5′-$C_dCG_dG_d$ (oligo-4). ○: oligonucleotide (5′-Seq(A)-Seq(B)), △: 5′-Seq(A)>p, ●: 5′-Seq(B), ▲: monomers, □, ■: unknown products.

tubings were tested to monitor the apparent reaction rate of oligo-17. The values of k_{app} of oligo-17 at 175 °C using PEEK and PTFE tubings were in good agreement (k_{app} = (4.33 ± 0.05) × 10^{-2} s^{-1} for PEEK, k_{app} = (4.31 ± 0.08) × 10^{-2} s^{-1} for PTFE), and no influence of the inner wall was confirmed.

Interesting trends were found from the values of k_{app} and the reaction curves. First, it was unexpected that the values of k_{app} for the -$C^{3'}pG_d$- sequence within five oligonucleotides would be dependent on the sequences at 150–200 °C. The first-order-rate plots demonstrate the difference between oligo-17 and oligo-11 (Fig. 5), where oligo-17 is 1.3–1.9-times more stable than oligo-17 at 80–200 °C. On the other hand, the values of k_{app} at 65–80 °C for oligo-17 and -23 were much smaller than those for oligo-4, -11, and -18, in which oligo-17 and -23 were 10–47-times more stable than oligo-4, -11, and -18. Second, the k_{app} values of $C^{2'}pG$ and $C^{3'}pG$ were a few-times smaller than those for the five oligonucleotides, in which $C^{2'}pG$ was somewhat more stable than $C^{3'}pG$. The difference in the stability between oligonucleotides and dinucleotides increased with the temperature. Third, the stability of the deoxyribose phosphodiester bond of C_dpG_d is greater than the ribose phosphodiester bond of $C^{2'}pG$ and $C^{3'}pG$, but the difference of the stability between deoxyribose and ribose decreases with the temperature.

In this study, imidazole was used to control the pH, since imidazole is important as a prebiotic molecule,[46,47] and is frequently used as a model of the active site of ribonuclease.[29–33,35,36] Besides, it was observed that histidine and a thermal copolymer including a histidine residue accelerate the degradation of 2-methylimidazolide of adenosine 5′-monophosphate.[48] Thus, some experiments on the influence of histidine were carried out; the pseudo-first-order rate constants are summarized in Table 1. It was detectable that the degradation of oligo-17 was somewhat accelerated in the presence of L- or D-histidine. There was less difference between L- and D-histidine.

Enhancement of the Stability of Oligonucleotides by Forming a Hairpin Structure at Low Temperatures. The hydrolytic stability of oligo-23 and oligo-17 notably increased below 65–80 °C. In order to test whether this was due to the formation of hairpin structure, the values of T_m for oligo-17,

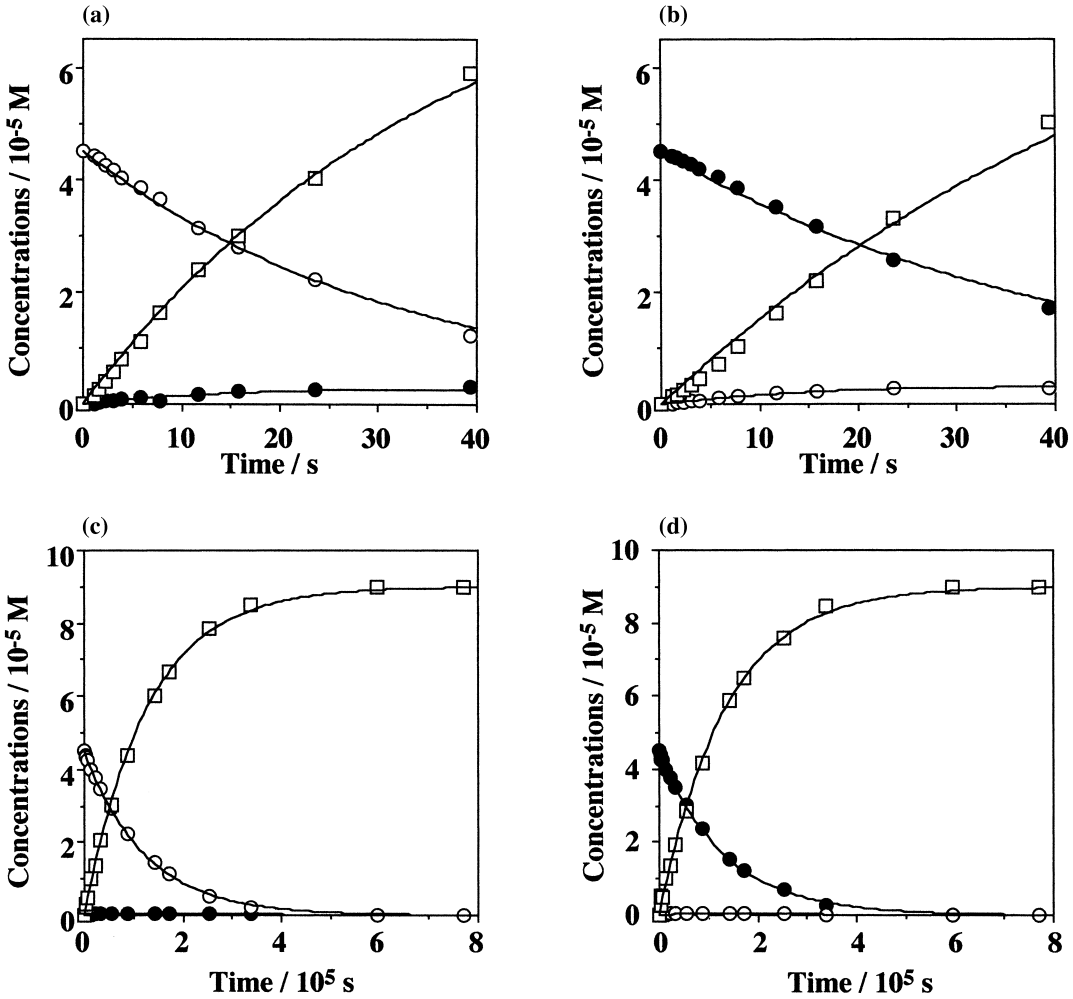

Fig. 4. Reaction curves for the degradation of $C^{2'}pG$ and $C^{3'}pG$. Reaction conditions are the same as shown in Fig. 2. ○: $C^{3'}pG$, ●: $C^{2'}pG$, □: monomers including 2′,3′-cyclic CMP, 2′-CMP, 3′-CMP, cytidine, and guanosine. Temperatures: (a), (b): 200 °C, (c), (d): 80 °C. The lines drawn through the experimental points were fit by SIMFIT.

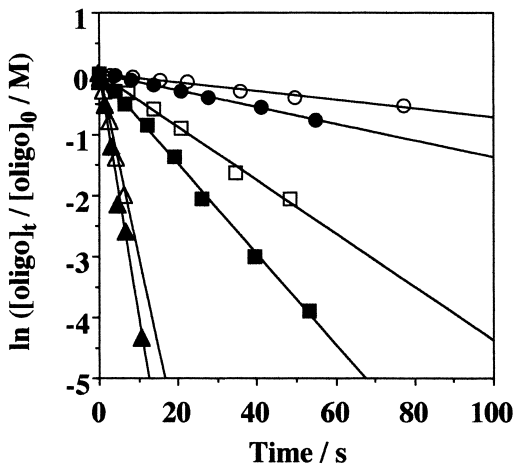

Fig. 5. Pseudo-first order rate plots for the degradation of oligo-17 and oligo-11. Reaction conditions are the same as shown in Fig. 2. Temperatures: ○, ●: 150 °C, □, ■: 175 °C, △, ▲: 200 °C. Oligonucleotides: ○, □, △: oligo-17, ●, ■, ▲: oligo-11.

-18, and -23 were determined using DSC. The T_m values in a buffer solution containing 0.1 M NaCl, 0.1 M $MgCl_2$, and 0.05 M imidazole (pH = 8.0) were 85.2 °C for oligo-23, 76.9 °C for oligo-18, and 76.0 °C for oligo-17. The T_m values are consistent with the number of base pairs which can possibly be formed within these oligonucleotides; the oligonucleotides form the hairpin structure with 9 base pairs for oligo-23 and 6 base pairs for oligo-18 and -17 (Fig. 1). The enhancement of the hydrolytic stability of oligo-23 at 65–80 °C and that of oligo-17 at 65 °C compared with oligo-4 and -11 are coincidence with the values of T_m. Because of the target -$C^{3'}pG_d$- sequence of oligo-17 and -23 is located within the double-helix of the hairpin structure, a higher hydrolytic stability than that in single-strand results. Besides, the stability of oligo-18 is not much different from that of oligo-4 and -11 at 65 °C. This fact indicates that the stability of the -$C^{3'}pG_d$- sequence in the hairpin loop is similar to that in a single strand.

Kinetic Dissection of Degradation of $C^{2'}pG$ and $C^{3'}pG$. During the degradation of $C^{2'}pG$ and $C^{3'}pG$, the interconversion between $C^{2'}pG$ and $C^{3'}pG$ was observed, as shown in Fig. 4. It is interesting that the extent of the interconversion in-

Table 2. Rate Constants for the Hydrolysis (k_{hy}/s^{-1}) and Interconversion (k_{int}/s^{-1}) of $C^{3'}pG$ and $C^{2'}pG$

Reactions	$C^{3'}pG \rightarrow C{>}p + G$	$C^{3'}pG \rightarrow C^{2'}pG$	$C^{2'}pG \rightarrow C{>}p + G$	$C^{2'}pG \rightarrow C^{3'}pG$
T/°C	(k_{hy}/s^{-1})	(k_{int}/s^{-1})	(k_{hy}/s^{-1})	(k_{int}/s^{-1})
65	$(3.58 \pm 0.17) \times 10^{-6}$	$(1.00 \pm 0.25) \times 10^{-7}$	$(3.70 \pm 0.16) \times 10^{-6}$	$(9.98 \pm 1.90) \times 10^{-8}$
80	$(7.85 \pm 0.06) \times 10^{-6}$	$(2.85 \pm 0.89) \times 10^{-7}$	$(7.39 \pm 0.05) \times 10^{-6}$	$(2.01 \pm 0.90) \times 10^{-7}$
150	$(1.12 \pm 0.01) \times 10^{-3}$	$(1.59 \pm 0.18) \times 10^{-4}$	$(9.39 \pm 0.11) \times 10^{-4}$	$(1.60 \pm 0.19) \times 10^{-4}$
175	$(5.30 \pm 0.04) \times 10^{-3}$	$(7.94 \pm 0.64) \times 10^{-4}$	$(3.90 \pm 0.04) \times 10^{-3}$	$(9.18 \pm 0.64) \times 10^{-4}$
200	$(2.62 \pm 0.03) \times 10^{-2}$	$(4.30 \pm 0.47) \times 10^{-3}$	$(1.83 \pm 0.03) \times 10^{-2}$	$(4.84 \pm 0.48) \times 10^{-3}$

Reaction conditions are the same as shown in Table 1.

creased with increasing temperature. According to the reaction curves, the model is assumed to be as shown in Eqs. II-1 – II-5, which is consistent with the degradation mechanism of dinucleoside monophosphate described in previous studies.[33,34] The reaction curves were fitted by SIMFIT.

(interconversion)

$C^{2'}pG \rightarrow C^{3'}pG$ (II-1)

$C^{3'}pG \rightarrow C^{2'}pG$ (II-2)

(hydrolysis)

$C^{2'}pG \rightarrow C{>}p + G$ (II-3)

$C^{3'}pG \rightarrow C{>}p + G$ (II-4)

$C{>}p \rightarrow Cyd$ (II-5)

Here, $k_{int,2}$, $k_{int,3}$, $k_{hy,2}$, and $k_{hy,3}$ indicate the rate constants for the reactions of Eqs. II-1–II-4, and C>p, G, and Cyd indicate cytidine 2′,3′-cyclic monophosphate, guanosine, and cytidine, respectively. The reactions were monitored from both $C^{2'}pG$ and $C^{3'}pG$, in which both reaction curves were simultaneously used for fitting calculations to determine the rate constants at each temperature. This procedure resulted in a better fit rather than to use data obtained from either $C^{2'}pG$ or $C^{3'}pG$. Since the yield of Cyd by the degradation of C>p was low, the rate constants for Eq. II-5 were not determined. The reaction rate constants are summarized in Table 2. A good fit to the experimental points was obtained for the degradation of $C^{2'}pG$ and $C^{3'}pG$ at 65–200 °C (Fig. 4). The values of k_{int} were smaller than those of k_{hy} at 65–200 °C.

Discussion

Stability of the Ribose Phosphodiester Bond at High Temperatures. The difference of the stability of oligonucleotides could be detected at 150–200 °C (Fig. 2, Table 1), and Arrhenius plots visualize the difference in the stability of the oligonucleotides, in which 3 types including (1) oligonucleotides involving -$C^{3'}pG_d$- sequence, (2) $C^{2'}pG$ and $C^{3'}pG$, (3) C_dpG_d are observed (Fig. 6). Moreover, it was unexpected that the difference among the five oligonucleotides could be detected. This finding is stimulating since the temperatures are much higher than T_m of the oligonucleotides; this fact may reflect that the surrounding sequence might affect the rate of degradation of the oligonucleotides based on some weak interactions at high temperatures. In general, the hydrolytic stability of the phosphodiester bond at low temperatures is affected whether within a double-strand or a single-strand.[39,40] Moreover, the hydrolytic stability is dependent on the length,[49,50] linkage geometry,[42] and the position even if the linkage is located within hairpin loops and a single strand.[40] The variation

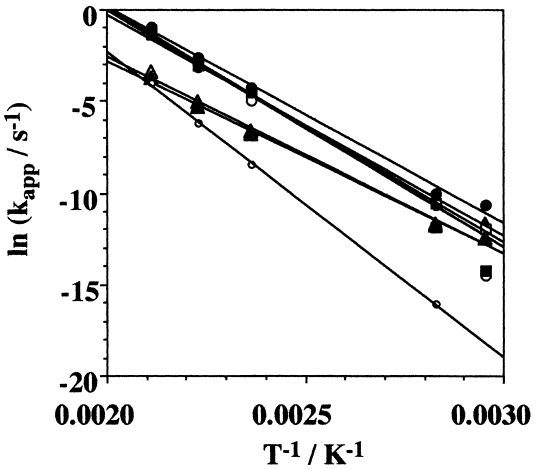

Fig. 6. Arrhenius plots of k_{app} for oligonucleotides and dinucleotides. ○: oligo-17, ●: oligo-11, □: oligo-18, ■: oligo-23, △: oligo-4; △: $C^{3'}pG$, ▲: $C^{2'}pG$, ○: C_dpG_d.

of k_{app} with different sequence at 150–200 °C is much smaller than that observed between single-strand and double-strand at low temperatures. In other words, the variation of k_{app} at 150–200 °C is as small as that observed within single-strand and/or a hairpin loop of oligonucleotides. Thus, it seems that the dependence of k_{app} on the surrounding sequences at high temperatures is substantially different from that caused by forming tertiary structures based on the conventional Watson–Crick model at low temperatures. The variation may occur with a small difference in the interactions between the oligonucleotides and the catalyst. In the present reaction, imidazole acts as a moderate catalyst for the degradation of oligonucleotides and dinucleotides. The acceleration by histidine for the degradation might reflect a difference in the interactions.[24] Moreover, a trend that $\Delta S^{\neq}_{app}$ increases with the length of the oligonucleotides indicates that the cleavage within long oligonucleotides is advantageous in an entropy change. This may be because the interaction between a catalyst with a long oligonucleotide is greater than that within a short one.

The Arrhenius plots for oligo-4 and oligo-11 indicate a simple linear relation (Fig. 6). However, the values of k_{app} of oligo-23 at 65 and 80 °C, and oligo-17 at 65 °C are notably smaller than that of other oligonucleotides. As mentioned above, this is consistent with the formation of a tertiary structure below the T_m temperature. Conclusively, the present study clearly demonstrated that the correlation between the stability and the tertiary structures reflects whether the target sequence exists within the double-helix. Besides, there is no convenient

technique for detecting tertiary structures at extremely high temperatures. Thus, the detection of a difference in the rate constants using the present monitoring method would be useful to determine tertiary structures at extremely high temperatures. In addition, the evaluation suggests that one should be careful to extrapolate the kinetic data from low temperatures to high temperatures.

In this study, imidazole was used to control the pH, where the pH value was adjusted at 8.0 at 25 °C. The pH values at high temperatures can be assumed from thermodynamic data of the dissociation constants of imidazole and water.[51,52] The estimated values of the pH are 6.15 at 150 °C, 5.92 at 175 °C, and 5.71 at 200 °C. It should be noted that the neutral pH ($[H^+] = [OH^-]$) value is pH 5.82 at 150 °C, 5.71 at 175 °C, and 5.63 at 200 °C, while the neutral pH is pH 7.0 at 25 °C. Thus, the pH values at 150–200 °C under the reaction conditions are regarded to be weakly basic. In addition, the extent of species of imidazole (Im^0 form) and imidazolium (HIm^+ form) are assumed to be 89% and 11% at 150–200 °C. This is consistent with the idea that the degree of hydrolysis is greater than that of interconversion for $C^{2'}pG$ and $C^{3'}pG$. Thus, the apparent rate constants for the degradation of the phosphodiester bond -$C^{3'}pG_d$- in oligonucleotides roughly show the rate constants of hydrolysis.

Here, it is known that imidazole acts as a moderate catalyst for the hydrolysis of the ribose phosphodiester bond. A number of studies were carried out as a ribonuclease model reaction.[31–33,35,36] Besides, the degradation of oligo-17 was somewhat accelerated with histidine at 150–200 °C. This may be due to the different catalytic abilities of imidazole and histidine. It is also interesting that both L- and D- histidine showed almost the same catalytic ability.

This study showed that the stability of $C^{2'}pG$ is somewhat greater than $C^{3'}pG$ at 150–200 °C (Table 1). The degradation of dinucleoside monophosphate was analyzed in order to investigate the ribonuclease model, in which no correlation was found between the base moiety structure and the stability of the phosphodiester bond.[34,38,53] A large difference in the stability of 3′,5′- and 2′,5′-linkages was only observed within a helical RNA.[54] Furthermore, it is surprising that the magnitude of k_{app} of $C^{2'}pG$ and $C^{3'}pG$ was notably smaller than that of other oligonucleotides at 150–200 °C. In a previous study, a similar trend was observed that the hydrolytic stability of polyuridylic acid is lower than that of 3′,5′-urydylyluridine monophosphate.[55] The 2′-OH group on 3′-terminal guanosine of $C^{2'}pG$ and $C^{3'}pG$, which is absent in the five oligonucleotides, may inhibit cleavage of the phosphodiester bond. Furthermore, it was observed that the 3′-terminal moiety structures of dinucleoside mono- and diphosphate affect the stability of the phosphodiester bond.[55] The 3′-OH and 2′-OH groups of guanosine in $C^{2'}pG$ and $C^{3'}pG$ are geometrically possible to approach the phosphodiester bond and the 2′-OH group of cytidine. This may be related to the greater stability of $C^{3'}pG$ and $C^{2'}pG$ than the oligonucleotides tested in this study.

The stability of the phosphodiester bond of C_dpG_d at low temperatures is much higher than that of the ribose phosphodiester bond, but becomes comparable at 200 °C. The relative stability of $C^{3'}pG$ and C_dpG_d increase with the temperature, in which the ratio of $k_{app}(C^{3'}pG)/k_{app}(C_dpG_d)$ was 80 at 80 °C and 1.9 at 200 °C. In previous studies, the differences in the stability of the phosphodiester bond between DNA and polyadenylic acid were also observed,[42,43] in which DNA was 3.9-times more stable than RNA at 80 °C.[43] Thus, the difference between $C^{2'}pG$ and $C^{3'}pG$ with C_dpG_d shown in the present study is greater than that observed in the previous study. This is probably due to several reasons, such as the length of nucleotides, the base moiety structures, and the buffer composition.

There was surprisingly fewer studies on the temperature dependence of the hydrolytic stability of the phosphodiester bond.[30,56] From the linear part of the lines of the Arrhenius plots, the apparent activation energy ($E_{a,app}$), the apparent enthalpy change ($\Delta H^{\ddagger}_{app}$), and the entropy change ($\Delta S^{\ddagger}_{app}$) were calculated (Table 3). A trend was found that $\Delta H^{\ddagger}_{app}$ and $\Delta S^{\ddagger}_{app}$ increased with the length of the oligonucleotides (Fig. 7). This trend is unexpected since no notable trend was observed between the values of k_{app} and the length of the oligonucleotides. Although the values of $\Delta H^{\ddagger}_{app}$ and $\Delta S^{\ddagger}_{app}$ involve cleavage and interconversion, the contribution of the cleavage should be greater than the interconversion. Thus, the increase in $\Delta H^{\ddagger}_{app}$ shows that the strength of the phosphodiester bond slightly increases with increasing length. Besides, the increase of $\Delta S^{\ddagger}_{app}$ indicates that long oligonucleotides at high temperatures take a more suitable conformation at the transition state than do the short oligonucleoides. Moreover, Fig. 7 clearly shows that the number of oligonucleotides selected in this study was sufficient to demonstrate the existence of differences in the stability

Table 3. Apparent Activation Parameters for the Degradation of Oligonucleotides and Dinucleotides

Nucleotides	$E_{a,app}$/kJ mol^{-1}	$\Delta H^{\ddagger}_{app}$/kJ mol^{-1}	$\Delta S^{\ddagger}_{app}$/J mol^{-1} T^{-1}
oligo-4	100 ± 3	97 ± 3	−57 ± 7
oligo-11	104 ± 2	101 ± 2	−45 ± 5
oligo-17	107 ± 4	104 ± 4	−42 ± 10
oligo-18	105 ± 1	102 ± 1	−45 ± 3
oligo-23	109 ± 5	105 ± 5	−36 ± 11
$C^{3'}pG$	90 ± 4	86 ± 4	−97 ± 9
$C^{2'}pG$	87 ± 4	84 ± 4	−105 ± 9
C_dpG_d	139 ± 2	135 ± 2	2 ± 5
oligo-17[a)]	102 ± 3	98 ± 2	−54 ± 5
oligo-17[b)]	102 ± 3	98 ± 3	−54 ± 6

Reaction conditions are the same as shown in Table 1.

Table 4. Activation Parameters for the Hydrolysis and Interconversion of $C^{3'}pG$ and $C^{2'}pG$

Reactions	$E_{a,int}$ or $E_{a,hy}$ /kJ mol^{-1}	$\Delta H^{\neq}_{int}$ or $\Delta H^{\neq}_{hy}$ /kJ mol^{-1}	$\Delta S^{\neq}_{int}$ or $\Delta S^{\neq}_{hy}$ /J mol^{-1} T^{-1}
$C^{3'}pG \rightarrow C{>}p + G$	88 ± 3	85 ± 3	−102 ± 9
$C^{3'}pG \rightarrow C^{2'}pG$	107 ± 3	103 ± 3	−76 ± 7
$C^{2'}pG \rightarrow C{>}p + G$	84 ± 3	82 ± 3	−113 ± 8
$C^{2'}pG \rightarrow C^{3'}pG$	110 ± 4	106 ± 4	−69 ± 11

Reaction conditions are the same as shown in Table 1.

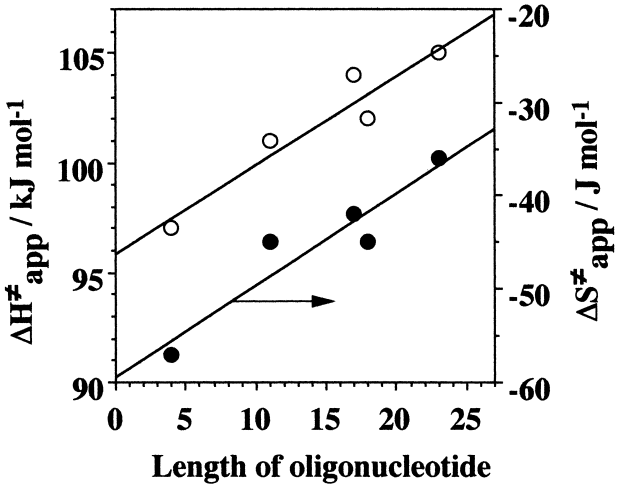

Fig. 7. Influence of length of the oligonucleotides for $\Delta H^{\neq}_{app}$ and $\Delta S^{\neq}_{app}$. ○: $\Delta H^{\neq}_{app}$, ●: $\Delta S^{\neq}_{app}$.

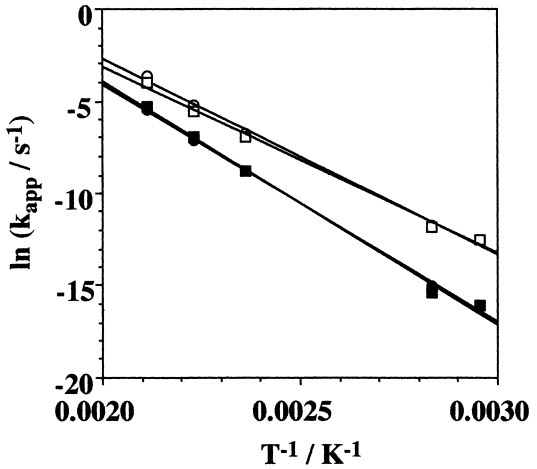

Fig. 8. Arrhenius plots of k_{hy} and k_{int} for $C^{2'}pG$ and $C^{3'}pG$. ○: $k_{hy,3}$ (hydrolysis of $C^{3'}pG$), ●: $k_{int,3}$ (interconversion of $C^{3'}pG$), □: $k_{hy,2}$ (hydrolysis of $C^{2'}pG$), ■: $k_{int,2}$ (interconversion of $C^{2'}pG$).

of the target sequence with different surrounding sequences. Besides, the values of $\Delta H^{\neq}_{app}$ and $\Delta S^{\neq}_{app}$ for the five oligonucleotides are greater than those for $C^{2'}pG$ and $C^{3'}pG$. This fact indicates that the lower stability of the oligonucleotides than that of $C^{2'}pG$ and $C^{3'}pG$ at 65–200 °C is due to the influence of an entropy change, since $\Delta H^{\neq}_{app}$ of the dinucleotides is smaller than that of the oligonucleotides. The fact that the values of $\Delta H^{\neq}_{app}$ and $\Delta S^{\neq}_{app}$ for C_dpG_d are greater than those for $C^{2'}pG$ and $C^{3'}pG$ indicates that the higher stability of DNA than RNA at below 200 °C is mainly due to the enthalpy change. Moreover, the influence of histidine is due to the decrease of both $\Delta H^{\neq}_{app}$ and $\Delta S^{\neq}_{app}$. It was shown that histidine is a somewhat stronger catalyst for the hydrolysis of the phosphodiester bond, which reflects the reduction of $\Delta H^{\neq}_{app}$. In addition, because histidine is a larger molecule than imidazole, this is also consistent with the small decrease of $\Delta S^{\neq}_{app}$ in the presence of histidine, in which a disadvantage may be assumed for the approach of histidine to oligo-17.

This study enabled us to determine k_{int} and k_{hy} for the degradation of $C^{2'}pG$ and $C^{3'}pG$ at high temperatures of over 100 °C (Table 2). Moreover, the activation parameters for the rate constants of k_{int} and k_{hy} was determined from the temperature dependence of k_{int} and k_{hy} (Fig. 8, Table 4). In this case, both values of k_{int} and k_{hy} are not much different between $C^{2'}pG$ and $C^{3'}pG$. The fact that the values of k_{hy} are greater than that of k_{int} is consistent with previous studies at low temperatures, in which it was deduced that imidazole (Im) and imidazolium (HIm^+) catalyze the hydrolysis and interconversion. The values of $E_{a,int}$ for $C^{2'}pG$ and $C^{3'}pG$ are somewhat higher than those of $E_{a,hy}$. The difference ($E_{a,int} - E_{a,hy}$) probably reflects the apparent activation energy ($E_{a,\psi}$) for the pseudorotation (ψ) through a pentacoordinate common intermediate of interconversion and hydrolysis. The magnitudes of $\Delta H^{\neq}_{hy}$ are greater than those of the $\Delta H^{\neq}_{int}$ values, and the magnitudes of $\Delta S^{\neq}_{hy}$ are smaller than those of $\Delta S^{\neq}_{int}$. A possible free-energy/reaction coordinate profile for the interconversion and hydrolysis for $C^{2'}pG$ and $C^{3'}pG$ is illustrated in Fig. 9, where the stability of $C^{2'}pG$ and $C^{3'}pG$ is almost equal and $E_{a,hy}$ is smaller than $E_{a,int}$. The free-energy profile clearly shows the relationship between the cleavage and interconversion through a common intermediate. Interconversion requires an extra activation energy for the pseudorotation of the pentacoordinate intermediate. Besides, the hydrolysis of C_dpG_d could not proceed through a pentacoordinate intermediate as in the hydrolysis of the ribose phosphodiester bond.

Although interconversion within the oligonucleotides was not detectable by the present HPLC method, interconversion should be considered to occur.[54] The reaction model can be applied for the degradation of oligonucleotides. For the cases of oligo-23 and oligo-17 at 65–80 °C, pseudorotation should be difficult, since the target sequence, -$C^{3'}pG_d$-, is located within a double-helical strand. In addition, the pentacoordinate intermediate is not favorable within the double-helical strand. Thus, oligo-23 and oligo-17 at 65–80 °C are more stable than other oligonucleotides. However, this is not the case within hairpin, since the stability of oligo-18 is similar to that of oligo-11 and oligo-4. Besides, $\Delta H^{\neq}_{app}$ and $\Delta S^{\neq}_{app}$, involving

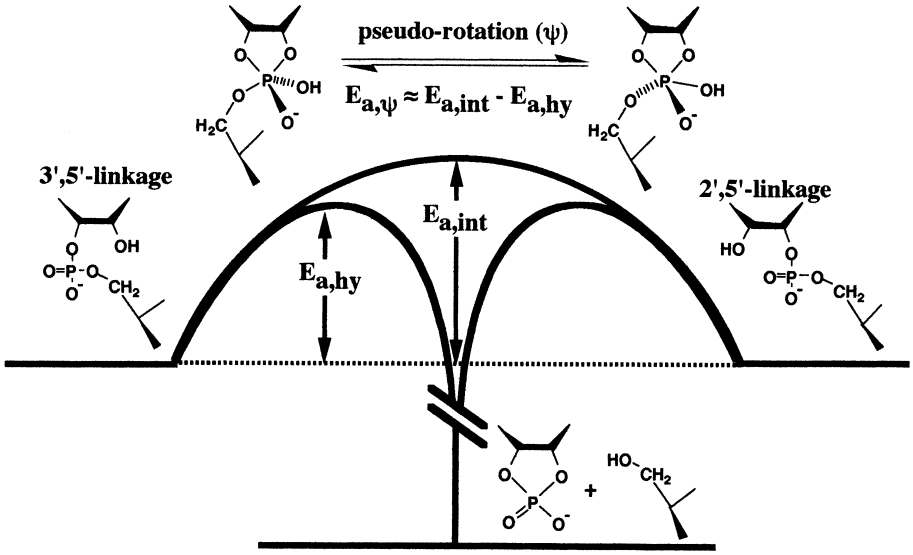

Fig. 9. A possible free-energy/reaction coordinate profile for the interconversion and hydrolysis for $C^{2'}pG$ and $C^{3'}pG$. $E_{a,hy}$: apparent activation energy of hydrolysis, $E_{a,int}$: apparent activation energy of interconversion. Deference of the apparent energy $E_{a,hy}$ and $E_{a,int}$ was very small between $C^{2'}pG$ and $C^{3'}pG$.

cleavage and pseudorotation, increase with increasing length of the oligonucleotides at high temperatures, as shown in Fig. 7. This fact indicates that the surrounding sequences affect the activation enthalpy and entropy for the formation of the pentacoordinate intermediate. This phenomenon is complicated, and it seems to be difficult to know the reason at the present time, since other conventional techniques for kinetics, which are used at low temperatures, are not applicable. Thus, further systematic investigations to accumulate the rate constants and activation parameters would be important. Conclusively, this study demonstrated the reality of a pentacoordinate common intermediate of hydrolysis and interconversion based on the temperature dependence of the kinetic analysis. In addition, the monitoring method has sufficient accuracy to collect activation parameters.

Implications on the Origin of Life. The half-lives are 2–3 s for oligonucleotides, 20–30 s for $C^{2'}pG$ and $C^{3'}pG$, and 40 s for C_dpG_d at 200 °C, and those are estimated to be 3–7 ms for oligonucleotide, 0.1–0.2 s for $C^{2'}pG$ and $C^{3'}pG$, and 10 ms for C_dpG_d at 350 °C. This fact indicates that the stability of nucleotides is very low at extremely high temperatures, and the emergence of the RNA world may have been difficult. The accumulation of RNA was not possible unless the prebiotic formation of RNA was much faster than the degradation if RNA was exposed under hydrothermal environments. If a specific inhibitor for the hydrolysis of RNA or an accelerator for the prebiotic formation of RNA existed, a possible temperature for the emergence of a RNA world should appear. To evaluate this consideration, the present data will be important to compare with the prebiotic formation rates in the future. Furthermore, the monitoring method will be absolutely useful to test the prebiotic formation of RNA under hydrothermal conditions.

In general, the differences in the hydrolytic stability should have been important under hydrolytic selection pressure of the oligonucleotides during chemical evolution. This study showed that the stability of the target sequence -$C^{3'}pG_d$- within the oligonucleotides is dependent on the surrounding sequences. The difference may be enhanced in the presence of inhibitors and accelerators, such as protein-like molecules and minerals. Besides, the stability of $C^{2'}pG$ is somewhat greater than that of $C^{3'}pG$. In previous studies on 2′,5′- and 3′,5′-linked dinucleoside monophosphate at low temperatures, no correlation between the base structure and the stability was observed.[34,38,53] Thus, the reason that 3′,5′-linked RNA selected in living organisms seems to be not directly related to the stability of the 2′,5′- and 3′,5′-linkages within dinucleoside monophosphate.

The stability of C_dpG_d is greater than $C^{2'}pG$ and $C^{3'}pG$ at 65–200 °C; this trend was also observed in previous studies at low temperatures. Although there were no data on the comparison of the stability of RNA and DNA at extremely high temperatures, the extrapolation of the temperature dependence of k_{app} showed that the stability of C_dpG_d becomes lower than that of $C^{3'}pG$ at over 218 °C. From this view point, RNA is capable of surviving more easily than DNA under extremely high temperatures, such as in hydrothermal vents in the deep ocean.

Conclusions. The hydrolytic stability of the ribose phosphodiester bond was successfully investigated using a new monitoring method, and oligonucleotides involving a single target sequence, -$C^{3'}pG_d$-. The apparent rate constants of hydrolysis at 65–200 °C and the activation parameters, $E_{a,app}$, $\Delta H^{\neq}_{app}$, and $\Delta S^{\neq}_{app}$, were determined. The magnitude of k_{app} of the target sequence, -$C^{3'}pG_d$-, was dependent on the surrounding sequences, and the activation parameters, $\Delta H^{\neq}_{app}$ and $\Delta S^{\neq}_{app}$, slightly increased with the oligonucleotide length. The apparent activation energy ($E_{a,\psi}$) could be estimated based on the difference of hydrolysis and interconversion, since $C^{3'}pG$ and $C^{2'}pG$ have similar stabilities. This demonstrated the reality of a common intermediate of hydrolysis and interconversion. Dinucleotides $C^{2'}pG$ and $C^{3'}pG$ are more stable than the -$C^{3'}pG_d$- sequence within oligonucleotides, but less stable than C_dpG_d. This study clearly demonstrated that the present tech-

nique for monitoring the hydrothermal reaction is useful and sufficiently accurate to obtain not only the rate constants, but also the activation parameters.

Accordingly, it was confirmed that the ribose phosphodiester bond is influenced within the surrounding sequences even under hydrothermal conditions. From the view of chemical evolution of RNA, the stability of 2′,5′- and 3′,5′-linkage is not directly related to the reason that 3′,5′-RNA was selected. DNA is stable at low temperatures, but becomes less stable than RNA at temperatures for sub- or super-critical water.

This research was supported by the Mazda Foundation's Research Grant 2000. The author greatly appreciates Professor. H. Fukada in College of Agriculture for the measurement of DSC and Professor T. Nakahara for the use of HPLC in Osaka Prefecture University. Professor G. von Kiedrowski generously provided SIMFIT.

References

1 J. B. Corliss, J. A. Baross, and S. E. Hoffman, *Ocean. Acta*, **4** (suppl.), 59 (1981).
2 J. A. Baross and S. E. Hoffman, *Origins of Life*, **15**, 327 (1985).
3 E. G. Nisbet, *Nature*, **322**, 206 (1986).
4 H. Yanagawa and F. Egami, *Proc. Jpn. Acad., Ser. B*, **54**, 331 (1984).
5 H. Yanagawa and K. Kojima, *J. Biochem.*, **97**, 1521 (1985).
6 E. Imai, H. Honda, K. Hatori, A. Brack, and K. Matsuno, *Science*, **283**, 831 (1999).
7 N. R. Pace, *Cell*, **65**, 531 (1991).
8 P. Forterre, *C. R. Sciences de la vie/Life sciences, Acad. Sci. Paris*, **318**, 415 (1995).
9 T. R. Cech, *Proc. Natl. Acad. Sci. U.S.A.*, **83**, 4360 (1986).
10 W. Gilbert, *Nature*, **319**, 618 (1986).
11 T. Inoue and L. E. Orgel, *J. Mol. Biol.*, **162**, 201 (1982).
12 H. Sawai, K. Kuroda, and H. Hojo, *Bull. Chem. Soc. Jpn.*, **62**, 2018 (1989).
13 J. P. Ferris and G. Ertem, *Science*, **257**, 1387 (1992).
14 K. Kawamura and J. P. Ferris, *J. Am. Chem. Soc.*, **116**, 7564 (1994).
15 A. Terfort and G. von Kiedrowski, *Angew. Chem., Int. Ed. Engl.*, **31**, 654 (1992).
16 A. D. Ellington and J. W. Szostak, *Nature*, **346**, 818 (1990).
17 R. H. White, *Nature*, **310**, 430 (1984).
18 R. Larralde, M. P. Robertson, and S. L. Miller, *Proc. Natl. Acad. Sci. U.S.A.*, **92**, 8158 (1995).
19 K. Kawamura, A. Yosida, and O. Matumoto, *Viva Origino*, **25**, 177 (1997).
20 K. Kawamura, N. Kameyama, and O. Matumoto, *Viva Origino*, **27**, 107 (1999).
21 K. Kawamura, *Nippon Kagaku Kaishi*, **1998**, 255.
22 K. Kawamura, *Chem. Lett.*, **1999**, 125.
23 K. Kawamura, *Bull. Chem. Soc. Jpn.*, **73**, 1805 (2000).
24 K. Kawamura, *Chem. Lett.*, **2001**, 1120.
25 K. Kawamura, *Nucl. Acids Res. Suppl.*, **1**, 239 (2001).
26 K. Kawamura and M. Umehara, *Bull. Chem. Soc. Jpn.*, **74**, 927 (2001).
27 H. L. Abrash, C.-C. S. Cheung, and J. C. Davis, *Biochemistry*, **6**, 1298 (1986).
28 T. Koike and Y. Inoue, *Chem. Lett.*, **1972**, 569.
29 M. R. Eftink and R. L. Biltonen, *Biochemistry*, **22**, 5134 (1983).
30 M. R. Eftink and R. L. Biltonen, *Biochemistry*, **22**, 5140 (1983).
31 R. Breslow and M. Labelle, *J. Am. Chem. Soc.*, **108**, 2655 (1986).
32 K. Taira, *Bull. chem. Soc. Jpn.*, **60**, 1903 (1987).
33 E. Anslyn and R. Breslow, *J. Am. Chem. Soc.*, **111**, 4473 (1989).
34 P. Jävinen, M. Oivanen, and H. Lönberg, *J. Org. Chem.*, **56**, 5396 (1991).
35 R. Breslow, *Proc. Natl. Acad. Sci. U.S.A.*, **90**, 1208 (1993).
36 R. Breslow, S. D. Dong, Y. Webb, and R. Xu, *J. Am. Chem. Soc.*, **118**, 6588 (1996).
37 C. Beckmann, A. J. Kirby, S. Kuusela, and D. C. Tickle, *J. Chem. Soc., Perkin Trans. 2*, **1998**, 573.
38 M. Oivanen, S. Kuusela, and H. Lönberg, *Chem. Rev.*, **98**, 961 (1998).
39 I. Zarorowska, S. Kuusela, and H. Lönberg, *Nucl. Acids Res.*, **26**, 3392 (1998).
40 I. Zagorowska, S. Mikkola, and H. Lönberg, *Helv. Chim. Acta*, **82**, 2105 (1999).
41 Y. Li and R. R. Breaker, *J. Am. Chem. Soc.*, **121**, 5364 (1999).
42 G. A. Soukup and R. R. Breaker, *RNA*, **5**, 1308 (1999).
43 J. Eigner, H. Boedtker, and G. Michaels, *Biochim. Biophys. Acta*, **51**, 165 (1961),
44 J. J. Butzow and G. L. Eichhorn, *Nature*, **254**, 358 (1975).
45 K. Ikehara, *Viva Origino*, **29**, 66 (2001).
46 R. Lohrmann and L. E. Orgel, *Nature*, **244**, 418 (1973).
47 L. E. Orgel and R. Lohrmann, *Acc. Chem. Res.*, **7**, 368 (1974).
48 K. Kawamura and K. Kuranoue, *Chem. Lett.*, **2001**, 1070.
49 R. Kierzek, *Nucl. Acids Res.*, **20**, 5073 (1992).
50 R. Kierzek, *Nucl. Acids Res.*, **20**, 5079 (1992).
51 H. C. Helgeson, *J. Phys. Chem.*, **71**, 3121 (1967).
52 H. Fukada and K. Takahashi, *Proteins: Structure, Function, and Genetics*, **33**, 159 (1998).
53 S. Kuusela and H. Lönberg, *Nucleosides Nucleotides*, **15**, 1669 (1996).
54 A. Usher and A. H. McHale, *Proc. Natl. Acad. Sci. U.S.A.*, **73**, 1149 (1976).
55 S. Kuusela and H. Lönberg, *J. Chem. Soc. Perkin Trans. 2*, **1994**, 2109.
56 K. Kawamura, submitted data for publication.